Revealing the role of environmental and mass quenching with SAG

S.A. Cora[1,2], T. Hough[1], C.A. Vega-Martínez[1] & A.A. Orsi[3]

[1] *Instituto de Astrofísica de La Plata, CONICET–UNLP, Argentina*
[2] *Facultad de Ciencias Astronómicas y Geofísicas, UNLP, Argentina*
[3] *Centro de Estudios de Física del Cosmos de Aragón, Teruel, Spain*

Contact / sacora@fcaglp.unlp.edu.ar

Resumen / Estudiamos la relevancia de procesos que dependen de la masa estelar o de la densidad del ambiente en la supresión de la formación estelar (SF, por sus siglas en inglés) de galaxias satélites pasivas a $z = 0$. Analizamos un catálogo de galaxias generado mediante la combinación del modelo semi-analítico SAG con la simulación MultiDark MDPL2. Encontramos que $M_\star \approx 10^{10.5}\,\mathrm{M}_\odot$ es la escala de masa estelar donde los procesos de supresión que dependen de la masa se vuelven importantes. Los procesos de ambiente dominan la supresión de SF de las satélites de baja masa ($M_\star \lesssim 10^{10.1}\,\mathrm{M}_\odot$). Las galaxias de alta masa tienen más probabilidad de experimentar un cese de su SF mientras son centrales, y aquéllas que permanecen activas luego de que se convierten en satélites son principalmente afectadas por procesos dependientes de la masa. El proceso completo de supresión de la SF es bien descrito por un escenario de retardo-luego-atenuación. Durante la primera fase, la tasa de formación estelar de las satélites disminuye de manera similar a la de las galaxias centrales en un tiempo que varía desde $\approx 3\,\mathrm{Gyr}$ a $\approx 1\,\mathrm{Gyr}$ para satélites de baja masa ($M_\star \approx 10^{10}\,\mathrm{M}_\odot$) y alta masa ($M_\star \approx 10^{11}\,\mathrm{M}_\odot$), respectivamente. Durante la segunda etapa, las tasas de enfriamiento del gas y, en consecuencia, de la SF disminuyen más abruptamente hasta que la satélite se vuelve pasiva. Esto ocurre en $\approx 1\,\mathrm{Gyr}$ independientemente de la masa estelar.

Abstract / We study the relevance of mass and environmental quenching to the star formation (SF) history of $z = 0$ passive satellite galaxies by analysing a galaxy catalogue generated from the combination of the semi-analytic model of galaxy formation SAG and the MultiDark simulation MDPL2. We find $M_\star \approx 10^{10.5}\,\mathrm{M}_\odot$ to be the stellar mass scale where mass quenching becomes important. Environmental processes dominate the SF quenching of low-mass satellite galaxies ($M_\star \lesssim 10^{10.1}\,\mathrm{M}_\odot$). High-mass galaxies are more likely to quench as centrals, and those that remain active after first infall are mainly affected by mass quenching. The whole quenching process is well described by a delay-then-fade quenching scenario. During the first phase of this two-stage process, the star formation rate of satellites declines as they were centrals in a delay time that ranges from $\approx 3\,\mathrm{Gyr}$ to $\approx 1\,\mathrm{Gyr}$ for low-mass ($M_\star \approx 10^{10}\,\mathrm{M}_\odot$) and high-mass ($M_\star \approx 10^{11}\,\mathrm{M}_\odot$) satellites, respectively. During the second stage, the gas cooling rate and, consequently, the star formation rate decay more abruptly until the satellite becomes passive. The time span of this fading phase is $\approx 1\,\mathrm{Gyr}$, largely independent of stellar mass.

Keywords / galaxies: clusters: general — galaxies: evolution — methods: numerical

1. Introduction

Passive galaxies are characterised by low levels of star formation (SF). The fractions of passive galaxies present strong correlations with stellar mass, environmental density (given either by local density or halo mass) and halo-centric radius, both locally (Wetzel et al., 2012) and at high redshift (Peng et al., 2010; Muzzin et al., 2012; Lin et al., 2014; Jian et al., 2017; Kawinwanichakij et al., 2017). Both central galaxies (those residing at the centres of their host dark matter haloes) and satellite galaxies (those orbiting in the group potential) are more likely to be quenched as their stellar masses increase. This dependence is stronger for the former and is produced by mass quenching (e.g. Peng et al., 2010; Henriques et al., 2017), which refers to self-regulating processes that contribute towards suppressing the SF and depend on stellar mass, such as feedback from active galactic nuclei (AGN) (e.g. Fabian, 2012; Beckmann et al., 2017) and stellar feedback (e.g. Hopkins et al., 2014; Chan et al., 2018). For a given stellar mass, the fraction of passive satellites increases with increasing halo mass as a result of the larger effect of environment-dependent physical processes like ram pressure stripping (RPS, Gunn & Gott, 1972), tidal stripping (TS, Merritt, 1983), and turbulent viscous stripping (Nulsen, 1982), i.e. environmental quenching.

The aim of this work is to contribute to our understanding of the relative role of mass and environmental quenching in $z = 0$ passive satellites. We use the latest version of our semi-analytic model of galaxy formation SAG (acronym for Semi-Analytic Galaxies; Cora et al., 2018, hereafter Paper I). The results obtained from the analysis of the galaxy population generated by this model regarding the current topic are exhaustively analysed in Cora et al. (2019, hereafter Paper II).

2. Model of galaxy formation

We use an hybrid model of galaxy formation that combines our semi-analytic model of galaxy formation SAG with the cosmological dark matter (DM) MULTIDARK simulation MDPL2, which is part of the COSMOSIM database*. This simulation follows the evolution of 3840^3 particles within a box of side-length $1\,h^{-1}\,\mathrm{Gpc}$, with a mass resolution $m_\mathrm{p} = 1.5 \times 10^9\,h^{-1}\,\mathrm{M}_\odot$ per DM particle (Klypin et al., 2016). It is consistent with a flat ΛCDM model characterised by Planck cosmological parameters: $\Omega_\mathrm{m} = 0.307$, $\Omega_\Lambda = 0.693$, $\Omega_\mathrm{B} = 0.048$, $n_\mathrm{s} = 0.96$ and $H_0 = 100\ h^{-1}$ km s^{-1} Mpc^{-1}, where $h = 0.678$ (Planck Collaboration et al., 2014). DM haloes have been identified with the ROCKSTAR halo finder (Behroozi et al., 2013a), and merger trees were constructed with CONSISTENTTREES (Behroozi et al., 2013b). SAG assigns one galaxy to each new detected halo in the simulation. Thus, each system of haloes contains a central galaxy associated to the main host halo. DM structures contained within them are subhaloes which host satellite galaxies. When subhaloes are no longer detected because of numerical resolution effects, the satellites are called orphans and their orbits are integrated taking into account mass loss by TS and dynamical friction effects.

SAG includes physical processes that affect the baryonic components. A hot gas halo is formed when the gas is shock-heated as it falls into the potential well of the DM halo. The radiative cooling of hot gas allows the formation of a rotationally supported disc from which quiescent SF takes place. The number of supernovae (SNe) of type Ia and II are estimated from the initial mass function (IMF) assumed; we adopt the Chabrier IMF (Chabrier, 2003). The energetic and chemical SN feedback contributes towards regulating the amount of stars formed and determining the metallicity of all baryonic components. Starbursts triggered by disc instabilities and/or galaxy mergers allow the formation of a stellar bulge and the growth of a central supermasive black hole (BH). Gas accretion onto BHs produces AGN feedback that reduces gas cooling in large (sub)haloes, preventing them from forming stars at late times. When the galaxy becomes a satellite, its hot gas halo is gradually removed by a robust model of environmental effects through the action of RPS and TS. These processes can also strip the cold gas disc when it is not longer shielded by the hot gas halo. The physical processes implemented in SAG are characterised by efficiencies and parameters that are tuned by using the Particle Swarm Optimization Technique (PSO, Ruiz et al., 2015) in order to satisfy a set of observational constraints.

3. Role of mass and environmental quenching in passive satellites

We classify a satellite as passive when its specific star formation rate (sSFR), defined as the ratio between its star formation rate (SFR) and its stellar mass, is lower that a certain threshold, i.e. $\mathrm{sSFR} < 10^{-10.7}\,\mathrm{yr}^{-1}$, following Brown et al. (2017). The predictions of MDPL2 regarding the fraction of currently passive satellites as a function of stellar mass, halo mass and halo-centric distance (see figs. 11 and 12 of Paper I) are in agreement with those inferred from observations (Wetzel et al., 2012). We extend this analysis considering the dependence of these fractions on the time of first infall z_infall, defined as the moment in which the galaxy becomes a satellite for the first time.

Fig. 1 presents the dependence on z_infall of the fraction of $z = 0$ passive satellites that are quenched at time of first infall, fq_infall. All satellites within main host haloes of present-day mass $\log(M_\mathrm{halo}[\mathrm{M}_\odot]) \geq 12.3$ are considered. They are grouped according to their local stellar mass (different lines). Low-mass satellites ($M_\star \lesssim 10^{10.1}\,\mathrm{M}_\odot$) have null or very small values of fq_infall regardless of z_infall, which indicates that they have not suffered mass quenching while being centrals. Self-regulating processes such as AGN feedback or disc instabilities do not quench the SF of these satellites neither prior to nor after infall because of their low stellar mass. Low-mass satellites are mainly affected by environmental processes which act for longer on galaxies that have been accreted earlier. Therefore, the fractions of $z = 0$ passive satellites, fq_z0, are larger for galaxies with higher z_infall (see figure 1 of Paper II).

High-mass galaxies ($M_\star \gtrsim 10^{10.5}\,\mathrm{M}_\odot$) are more likely to be quenched as centrals as arises from the higher values of fq_infall for more massive galaxies, at fixed z_infall (Fig. 1). Moreover, for a given stellar mass range, fq_infall is larger for galaxies that have been accreted at later times (lower z_infall). This is explained by the combination of the stellar mass growth of a galaxy prior to infall and the time elapsed under the action of mass quenching processes while being central. After infall, the SF quenching of high-mass satellites continues to be dominated by mass quenching processes.

These results allow us to conclude that environmental processes dominate the SF quenching of low-mass satellites, and that $M_\star \approx 10^{10.5}\,\mathrm{M}_\odot$ is the mass scale where mass quenching becomes important. This picture is consistent with the results of previous works (van den Bosch et al. 2008, Peng et al. 2010, W13, Lin et al. 2014, Kawinwanichakij et al. 2017, Cochrane & Best 2018).

4. Delay-then-fade quenching scenario

The evolution of the sSFR of $z = 0$ passive satellites that were star-forming at infall indicates that their SF quenching process consists of two stages. During the first one, the rates of gas cooling experience a reduction of ≈ 50 percent with respect of their values at infall ($\approx 30 - 40\,\mathrm{M}_\odot\,\mathrm{yr}^{-1}$). These values allow the satellites to sustain high levels of SF so that their SFR declines gradually as if they were centrals (delay phase). During the second stage, the gas cooling rates and, consequently, the SFR decline faster until the satellites become passive (fading phase). The cooling rates reach values as low as $\approx 5\,\mathrm{M}_\odot\,\mathrm{yr}^{-1}$ by the time the satellites are quenched, which shows that the halt of cold gas supply is not a necessary condition for the onset of the SF

*https://www.cosmosim.org

quenching as assumed in the strangulation quenching scenario (Peng et al., 2015).

The origin of the decrease of the gas cooling rates depends on the stellar mass. In low-mass satellites, this decrease occurs because of the gradual removal of the hot gas halo through RPS; the fraction of the hot gas with respect to the total baryonic component of the satellites is reduced to $f_{\rm hot} \approx 0.5$ by the time they become passive. On the other hand, high-mass satellites keep a larger fraction of their hot gas reservoir by that time ($f_{\rm hot} \gtrsim 0.7$), and the cooling rates are reduced as a consequence of AGN feedback. Without an efficient replenishment through gas cooling, the cold gas disc is gradually depleted mainly by SF and/or removal through SN feedback. RPS of the cold gas does not play any role in the fading of SF. It only acts on a small fraction of satellites ($\approx 5-15$ percent) that have lost their protective hot gas halo before being quenched. This process may also contribute towards reducing even more the cold gas fraction after SF quenching.

The length of time of the delay and fading phases ($t_{\rm q,delay}$ and $t_{\rm q,fade}$, respectively) are comprised within the quenching time $t_{\rm q}$, which characterises the whole quenching process. The latter is estimated as the period of time elapsed since the galaxy is accreted and the moment in which it becomes passive. Median values of $t_{\rm q}$ are smaller for more massive galaxies: $t_{\rm q} \approx 4-5$ Gyr for $M_\star \approx 10^{10}\,{\rm M}_\odot$ and ≈ 2 Gyr for $M_\star \approx 10^{11}\,{\rm M}_\odot$, consistent with results from Wetzel et al. (2013). The time span of the delay and fading phases are obtained by considering the physically motivated cooling-rate based criterion, i.e. we define $t_{\rm q,fade}$ as the period of time elapsed since the gas cooling rate is reduced to half the value it has at infall until the satellite becomes passive. We find median values of $t_{\rm q,fade} \approx 1$ Gyr, regardless of stellar mass. Therefore, median values of the delay time range from $t_{\rm q,delay} \approx 3$ Gyr for low-mass satellites ($M_\star \lesssim 10^{10}\,{\rm M}_\odot$) to ≈ 1 Gyr for high-mass ones ($M_\star \approx 10^{11}\,{\rm M}_\odot$). The comparison of the length of time of the two phases for a given stellar mass shows that our model is only consistent with the delay-then-rapid quenching scenario proposed by Wetzel et al. (2013) for low-mass satellites. This scenario does not represent the situation of high-mass satellites whose delay and fading phases have similar lengths of time. Hence, we propose a *delay-then-fade* quenching scenario to fairly describe all the possible situations.

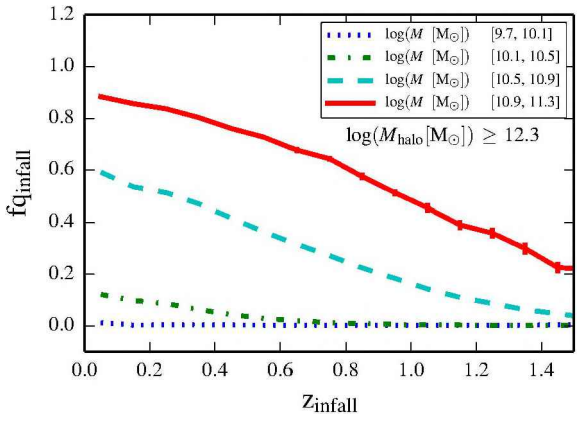

Figure 1: Fraction of $z = 0$ passive satellites that are quenched at first infall, $fq_{\rm infall}$, as a function of the redshift at infall, $z_{\rm infall}$. All satellites within main host haloes of present-day mass $\log(M_{\rm halo}[{\rm M}_\odot]) \geq 12.3$ are included. They are grouped according to their $z = 0$ stellar mass (different lines). Error bars show the 68 percent bayesian confidence interval estimated following Cameron (2011).

Acknowledgements: The authors thank the referee for useful comments and suggestions. They gratefully acknowledge the Gauss Centre for Supercomputing e.V. (www.gauss-centre.eu) and the Partnership for Advanced Supercomputing in Europe (PRACE, www.prace-ri.eu) for funding the MultiDark simulation project by providing computing time on the GCS Supercomputer SuperMUC at Leibniz Supercomputing Centre (LRZ, www.lrz.de). The MDPL2 simulation has been performed under grant pr87yi. This work was done in part using the Geryon computer at the Center for Astro-Engineering UC, part of the BASAL PFB-06, which received additional funding from QUIMAL 130008 and Fondequip AIC-57 for upgrades. SAC acknowledges funding from *Consejo Nacional de Investigaciones Científicas y Técnicas* (CONICET, PIP-0387), *Agencia Nacional de Promoción Científica y Tecnológica* (ANPCyT, PICT-2013-0317), and *Universidad Nacional de La Plata* (G11-124), Argentina. TH and CVM acknowledge CONICET, Argentina, for their supporting fellowships. AO acknowledges support from project AYA2015-66211-C2-2 of the Spanish *Ministerio de Economía, Industria y Competitividad.* This project has received funding from the European Union's Horizon 2020 Research and Innovation Programme under the Marie Sklodowska-Curie grant agreement No 734374.

References

Beckmann R.S., et al., 2017, MNRAS, 472, 949
Behroozi P.S., Wechsler R.H., Wu H.Y., 2013a, ApJ, 762, 109
Behroozi P.S., et al., 2013b, ApJ, 763, 18
Brown T., et al., 2017, MNRAS, 466, 1275
Cameron E., 2011, PASA, 28, 128
Chabrier G., 2003, PASP, 115, 763
Chan T.K., et al., 2018, MNRAS, 478, 906
Cochrane R.K., Best P.N., 2018, MNRAS, 480, 864
Cora S.A., et al., 2018, MNRAS, 479, 2
Cora S.A., et al., 2019, MNRAS, 483, 1686
Fabian A.C., 2012, ARA&A, 50, 455
Gunn J.E., Gott J.R.I., 1972, ApJ, 176, 1
Henriques B.M.B., et al., 2017, MNRAS, 469, 2626
Hopkins P.F., et al., 2014, MNRAS, 445, 581
Jian H.Y., et al., 2017, ApJ, 845, 74
Kawinwanichakij L., et al., 2017, ApJ, 847, 134
Klypin A., et al., 2016, MNRAS, 457, 4340
Lin L., et al., 2014, ApJ, 782, 33
Merritt D., 1983, ApJ, 264, 24
Muzzin A., et al., 2012, ApJ, 746, 188
Nulsen P.E.J., 1982, MNRAS, 198, 1007
Peng Y., Maiolino R., Cochrane R., 2015, Nature, 521, 192
Peng Y.j., et al., 2010, ApJ, 721, 193
Planck Collaboration, et al., 2014, A&A, 571, A16
Ruiz A.N., et al., 2015, ApJ, 801, 139
van den Bosch F.C., et al., 2008, MNRAS, 387, 79
Wetzel A.R., Tinker J.L., Conroy C., 2012, MNRAS, 424, 232
Wetzel A.R., et al., 2013, MNRAS, 432, 336